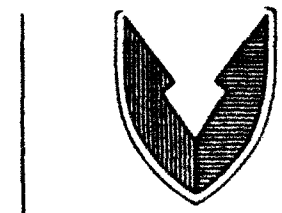

Research and Development Technical Report
SLCET-TR-91-11

Magnetic Field Source for Bi-Chambered Electron Beam Devices

Anup S. Tilak, Douglas J. Basarab,
Herbert A. Leupold and Ernest Potenziani II

November 1992

U.S. ARMY RESEARCH LABORATORY
Electronics and Power Sources Directorate
Fort Monmouth, NJ 07703-5601

NOTICES

Disclaimers

The findings in this report are not to be construed as an official Department of the Army position, unless so designated by other authorized documents.

The citation of trade names and names of manufacturers in this report is not to be construed as official Government indorsement or approval of commercial products or services referenced herein.

REPORT DOCUMENTATION PAGE

Form Approved
OMB No. 0704-0188

1. AGENCY USE ONLY (Leave blank)	2. REPORT DATE	3. REPORT TYPE AND DATES COVERED
	November 1992	Technical Report

4. TITLE AND SUBTITLE
MAGNETIC FIELD SOURCE FOR BI-CHAMBERED ELECTRON BEAM DEVICES

5. FUNDING NUMBERS
PE: 1L1
PR: 61102
TA: AH47

6. AUTHOR(S)
Anup S. Tilak, Douglas J. Basarab, Herbert A. Leupold, and Ernest Potenziani II

7. PERFORMING ORGANIZATION NAME(S) AND ADDRESS(ES)
US Army Research Laboratory
Electronics and Power Sources Directorate (EPSD)
ATTN: AMSRL-EP-EC-H
Fort Monmouth, NJ 07703-5601

8. PERFORMING ORGANIZATION REPORT NUMBER
SLCET-TR-91-11

9. SPONSORING/MONITORING AGENCY NAME(S) AND ADDRESS(ES)

10. SPONSORING/MONITORING AGENCY REPORT NUMBER

11. SUPPLEMENTARY NOTES

12a. DISTRIBUTION/AVAILABILITY STATEMENT
Approved for public release; distribution is unlimited.

12b. DISTRIBUTION CODE

13. ABSTRACT *(Maximum 200 words)*

Certain gyro-type electron beam devices require two tandem coaxial chambers with different uniform axial magnetic fields in their interiors. Therefore, there is a step in the field profile in the vicinity of the junction of the two chambers, which are sometimes of different diameter as well. An electric solenoid is usually employed to furnish such a field but the sources are bulky, cumbersome, and consumptive of energy, and provide only rough approximations to the ideal field profile. This report describes a permanent magnet field source that was designed to provide a constant axial field of 2 kOe in the larger of the two chambers and 0.5 kOe in the smaller. The basic field is provided by two tandem permanent magnet solenoids.

The rather broad transition between the field values in the two chambers is considerably narrowed (approximately 50 percent) by the placement of a radially magnetized ring internal to the junction of the two solenoids. The field profile can be made to conform to that specified to within a few percent by addition of two axially magnetized rings.

14. SUBJECT TERMS
magnetic field source; permanent magnet solenoid; bi-chambered gyrotrons; sharpening of magnetic field steps

15. NUMBER OF PAGES
22

16. PRICE CODE

17. SECURITY CLASSIFICATION OF REPORT	18. SECURITY CLASSIFICATION OF THIS PAGE	19. SECURITY CLASSIFICATION OF ABSTRACT	20. LIMITATION OF ABSTRACT
Unclassified	Unclassified	Unclassified	UL

TABLE OF CONTENTS

LIST OF FIGURES

INTRODUCTION

A variety of military radar and communication systems require strong signals of mm and near mm wave radiation. Sources and amplifiers of the gyrotron type are very attractive for such applications, but they tend to be quite large and require massive, bulky electric solenoids to furnish the magnetic field for the guidance of their electron beams. For example, a prototypical bi-chambered gyroamplifier designed at EPSD (Electronics and Power Sources Directorate) employs magnetic fields of 2.0 kOe and 0.5 kOe in cylindrical chambers that are respectively 25.4 cm and 15.24 cm in diameter. The electric solenoids (Figure 1) that provide these fields weigh approximately 1700 lbs and their accompanying power supplies weigh an additional 25 lbs for a total of 1725 lbs. Such cumbersome arrangements do not lend themselves readily to military applications that require portability and therefore their use is restricted to fixed stations, ships or very large trucks. To ameliorate these difficulties, a study was made at EPSD to examine the feasibility of designing a permanent magnet field source to replace the presently used electric solenoids.

AXIAL FIELD PERMANENT MAGNET SOLENOID

An obvious possibility for the construction of the required device is the tandem arrangement of two single chambered devices such as those previously invented at EPSD and GE which are pictured in Figure 2. To provide a passage for electron beam transit, the chamber walls at the juncture must be pierced so that one obtains a bi-chambered structure like that of Figure 3. The structure of figure 2A is composed of three primary parts: 1) a supply magnet in the form of an axially magnetized hollow cylinder which produces the field in the cylindrical working space; 2) iron pole pieces at each end of the supply magnet cylinder; which complete the magnetic circuit. (the flux path from supply magnets through the pole pieces into the working space is shown in Figure 4A); and 3) the cladding, which surrounds the rest of the structure and which confines the flux to the working space. In Figures 2 and 3 the small arrows represent the directions of magnetization of the constituent permanent magnets and the large arrows denote the direction of the required magnetic field.

For the mono-chambered device, Figure 4A summarizes the calculation of the supply magnet thickness from the specified field and dimensions of the working space. From Ampere's Law and the assumption of perfect flux confinement, we have

$$H_m = H_w \tag{1}$$

where H_m is the field within the supply magnet and H_w is the field in the working space. Equating the flux inside the supply magnet to the flux within the working space, we have

$$B_m A_m = H_w A_w \tag{2}$$

where

$$B_m = H_m + B_R \tag{3}$$

and A_m and A_w are the cross-sectional area of the supply magnet and of the working space respectively. Substituting for B_m in Eq. (2) and solving for A_m we obtain

$$A_m = A_w/(B_R/H_w) \tag{4}$$

Equation (4) is written in the form shown to obviate the need to include the sign of H_m, since $H_m<0$. The outer radius of the supply magnet is determined by A_m through the expression

$$A_m = \pi(r_o^2 - r_i^2) \tag{5}$$

where r_o and r_i are the outer and inner radius of the supply magnet respectively.

To determine cladding thickness, we employ the circuital form of Ampere's Law, which states that in the absence of linking currents, the integral of the dot product of H and dl around a closed path is zero. In Figure 4B, dl is an infinitesimal length in the direction of the closed path ABCDA; H is the magnetic field along each leg. Along path AB, $H=H_m$; along path BC and CD, $H=0$. Since we assume no flux leakage, there is no field outside the structure. Hence, the change in magnetic potential delta, ΔU, is zero along the path BCD.

Therefore, the change in magnetic potential along the path DA must be equal and opposite to the change in magnetic potential along the path AB.

Therefore,

$$H_w x = H_d d \tag{6}$$

where H_d is the radial field in the cladding.

Since, by hypothesis, no flux passes from A to D, the flux density B must be zero and the field H must equal the coercive force H_c. Therefore, we may substitute H_c for H_d and H_m for H_W in Eq. (6) which then becomes

$$H_c d - H_m x = 0 \tag{7}$$

from which

$$d = H_m x/H_c \tag{8}$$

where H_c is the coercivity, d is the distance DA (or the cladding thickness at any point x), and x is the distance BA. Equation (8) yields the cladding thickness at any point along the device for $0 \leq x \leq L$ where L is the total length of the structure. The thickness of the end cladding is the same as the maximum cladding thickness, $t_c(max)$, calculated for x=L in Eq. (8).

Next, we find the thickness of the pole pieces by equating the flux in the working space to the flux, ϕ_w traversing the circular band that forms the circumference of the pole piece. The result is:

$$\phi_w = H_w A_w = 2\pi r_w B_p$$
$$t_p = H_w A_w / 2\pi r_w B_p \qquad (9)$$

If the pole piece is to be unsaturated, Bp must be no larger than B_s , the saturation induction of the pole piece material. In our case, B_s is the saturation induction of iron (20 kG), r_w is the radius of the working space, and t_p is the thickness of the pole piece. To build in a safety factor to prevent local saturation, we multiply the resulting minimal thickness by 2 and obtain.

$$t_p = H_w A_w / 2\pi r_w \qquad (10)$$

with the determination of these dimensions, the design of the single chambered device is completed.

For a field of 0.5 kOe and a working space length of 30.5 cm (12 inches), a mono-chambered device was designed and is shown in Figure 5.

The bi-chambered device of Figure 3 is obtained by placing a similar design that produces 2 kOe in a working space of 61.0 cm length and 25.4 cm diameter in tandem with that of Figure 5.

From the dimensions of the structure, we obtain its volume and mass. All calculations were performed for a structure composed of $SmCo_5$ with a density of 8.3 gm/cm^3 and a remanence of 10 kG.

PARAMETRIC VARIATION OF CLADDING REMANENCE

A finite element analysis of the magnetic field produced by the basic bi-chambered permanent magnet solenoid shows that the field deviates considerably at both ends of the device (Figure 6). This behavior results from leakage arising from cladding imperfections at each end of the structure; the ideal cladding configuration in this area is impossible to obtain and approximations are therefore necessary.

To compensate for this leakage, the cladding is increased parametrically in the same proportion as the deviation in magnetic field. This modification was accomplished by a subdivision of the cladding. The remanence of the cladding around the gun chamber was then increased linearly from 10 kG to 11.5 kG towards the junction, and the remanence of the cladding of the circuit chamber was increased linearly from 10 kG to 12 kG with progression away from the junction.

EFFECT OF A RADIALLY MAGNETIZED RING ON THE FIELD TRANSITION BANDWIDTH

The field transition between the chambers of the structure (Figure 3) is narrower than that in the

solenoid of Figure 1. The change in magnetic field from 2 kOe to 0.5 kOe occurs over a distance of 32.5 cm, which is 35% of the length of the working space.

The magnetic field produced by a radially magnetized ring (see Appendix A or B) should reduce the transition width at the junction, if the magnetic field resulting from the above ring placed around the junction of the solenoids follows the superposition principle. Figure 7 shows how the transition width would be reduced by the placement of such a ring. Figure 8 (structure C) shows the positioning of the ring outside the solenoid, and Figure 9 shows the resulting magnetic field profile. Figure 10 shows a radially magnetized ring inside the working space, and the resulting magnetic field profile is depicted in Figure 11.

The dimensions of the ring were determined from the transition width (length of the ring is half the transition width) and the required correction in the magnetic field along the transition. The structure with the ring inside the working space is more suitable since the iron pole piece at the junction of the device interferes less with the flux lines from the ring than in the structure where it is placed outside, and therefore more nearly approximates ideal superposition.

EFFECT OF AN AXIALLY MAGNETIZED RING ON THE REDUCTION OF FIELD GRADIENT IN THE LARGER CHAMBER

The gradient in the circuit chamber originates from two sources: 1) flux leakage (due to imperfect cladding at the ends), 2) the presence of the radially magnetized ring inside the working space.

This field gradient can be reduced with strategically placed axially magnetized rings. The same superposition principle discussed above was used to determine the location and sizes of the rings needed. One such ring, placed outside, at the end of the circuit chamber (as structure D in Figure 12), increases the ripple in the field. Another ring was then placed inside the circuit chamber to reduce the ripple in the magnetic field arising from the previous adjustment.

COMPARISON OF PERMANENT MAGNET DEVICE WITH ELECTRIC SOLENOID

Comparison of Figures 13 and 14 shows clearly that the electric solenoid in Figure 14 does not maintain the desired field strength over an appreciable distance in either chamber. In contrast, the permanent magnet solenoid maintains a steady field slightly above 2 kOe in the circuit chamber over approximately 45 cm of the 60 cm length. In the gun chamber, a constant field of 0.45 kOe is maintained over the 30 cm length. In this respect, the permanent magnet structure is clearly superior to the electric field solenoid with respect to both field stability and uniformity.

In the electric solenoid, the transition band spans a length of 50 cm, whereas, in the permanent magnet alternative, the transition is only 18 cm wide. Clearly, when sharp transitions are required, the permanent magnet solenoid is preferable.

The structure is slightly heavier than the electric solenoid, 1700 pounds and 1675 pounds, respectively. Although, the structures weigh approximately the same, the permanent magnet structure is more portable; it requires no power supply, cables or other accessories.

SUMMARY AND CONCLUSIONS

A permanent magnet configuration produces a more uniform field and narrower transition than its electric solenoid counterpart. In addition, it is lighter and independent of electric power source and nonconsumptive of energy. In applications where these factors are a primary concern, the permanent magnet structure is the obvious choice. Overall, the permanent magnet alternative is superior to the electric solenoid.

LITERATURE CITED

1. D. J. Basarab, R. D. Finnegan, H. A. Leupold, "Permanent Magnet Structures for Magnetic Czochralski Crystal Growth," LABCOM Technical Report, SLCET-TR-88-12, October 1988.

2. W. Neugebauer and E. M. Branch, "Applications of Cobalt-Samarium Magnets to Microwave Tubes," Technical Report, Microwave Tube Operation, General Electric (15 March 1972).

3. John P. Clarke, Herbert A. Leupold, "Shaping Cylindrically Symmetric Magnetic Fields with Permanent Magnets," IEEE Transactions on Magnetics, Vol. MAG-22, No. 5, Sept 1986.

APPENDIX A. AXIALLY MAGNETIZED RING

Figure 15 shows the cross section of an axially magnetized ring, where a and b are the inner and outer radii of the ring, and c is its length. The pole density is given by magnetization

$$\sigma = M = B_R/4\pi \tag{A-1}$$

where B_R is the remanence of the ring.

The magnetic field H at any point along the axis of the ring is given by

$$H = H_1 + H_2 \tag{A-2}$$

where H_1 is the magnetic field from the positive poles and H_2 the magnetic field from an equivalent negative pole distribution. According to Coulomb's Law, the magnetic field at any point a distance r, away from the ring, along its axis is given by

$$H_1 = \int_a^b \frac{2\pi M \cos\theta}{r^2} d\rho \tag{A-3}$$

where $d\rho$ is the thickness of the circular charge element a distance ρ away from the axis and r is the distance from the charge element to a given point on the axis. The cosine term reflects the contribution from the longitudinal component alone. The transverse components cancel.

By analogy, a similar expression can be written for H_2, the contribution from the negative plate, with M replaced by $-M$.

Summation of H_1 and H_2 subsequent to integration, yields

$$H = 0.5B_R\Big[x\left(x^2+a^2\right)^{-1/2} - x\left(x^2+b^2\right)^{-1/2} + (x+c)\left\{(x+c)^2+b^2\right\}^{-1/2} + \ldots \\ -(x+c)\left\{(x+c)^2+a^2\right\}^{-1/2}\Big]^{-1} \tag{A-4}$$

where x is the distance of the face along the axis.

APPENDIX B. RADIALLY MAGNETIZED RING

Figure 16 shows a cross section of a radially magnetized ring, where a, b and c are the dimensions as stated above. The surface pole density is calculated with Eq.(A-l) as before. The magnetic field H at any point along the axis of the ring is a combination of three contributions,

$$H = H_1+H_2+H_3 \tag{B-1}$$

where H_1 and H_2 are the respective contributions from the positive and negative surface poles and H_3 is the contribution from a net volume poles distribution which is given by:

$$\rho = \nabla \cdot \vec{M} \tag{B-2}$$

Again, Coulomb's Law yields the field from a positive pole element of length dx, a distance y away from the ring along its axis the contribution from the volume charge, H_3, is determined by insertion of the volume charge density in Coulomb's law.

$$H_3 = 0.5B_R \ln\left[\frac{b+\sqrt{b^2+(y-c)^2}}{a+\sqrt{a^2+(y-c)^2}} \cdot \frac{a+\sqrt{a^2+y^2}}{b+\sqrt{b^2+y^2}}\right] \tag{B-3}$$

where a is the inner radius of the ring, b is the outer radius, c is the ring thickness in the axial direction and y is the distance of the center of the ring to the point where the field is being calculated.

The total magnetic field H results when the fields due to the volume and surface poles are added:

$$H = 0.5B_R\left[\frac{a}{\sqrt{a^2+(y-c)^2}} - \frac{a}{\sqrt{a^2+y^2}\sqrt{b^2+(y-c)^2}} - \frac{b}{b^2+y^2}\right.$$
$$\left. + \ln\left[\frac{\left(b+\sqrt{b^2+(y-c)^2}\right)\cdot\left(a+\sqrt{a^2+y^2}\right)}{\left(a+\sqrt{a^2+(y-c)^2}\right)\cdot\left(b+\sqrt{b^2+y^2}\right)}\right]\right] \tag{B-4}$$

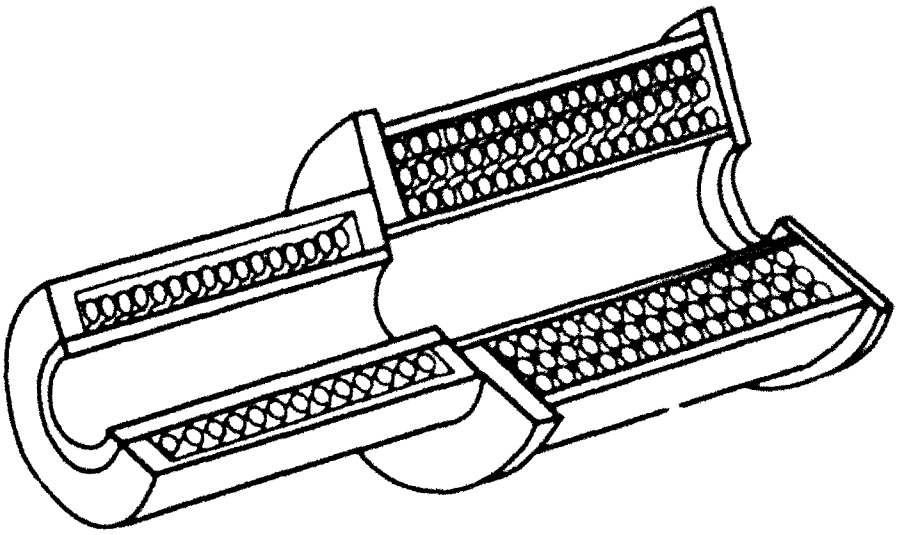

Figure 1. Structure A: Double electric solenoid gyrotron magnet.

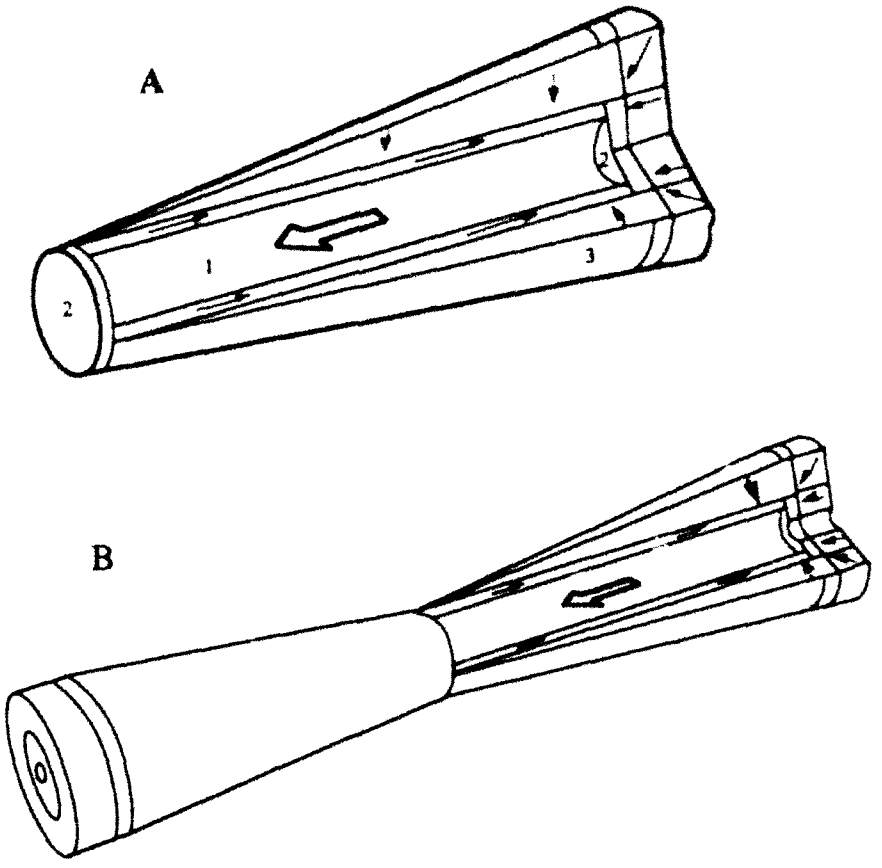

Figure 2. Two forms of permanent magnet solenoid: (A) the Neugebauer-Branch version, (B) the EPSD revision. Type B produces the same field in the same space as type A with less than half the mass. However, passage of an axial electron beam through a tunnel at either end of a type B structure entails a reversal of magnetic field. When such a reversal is undesirable, a type A structure must be used.

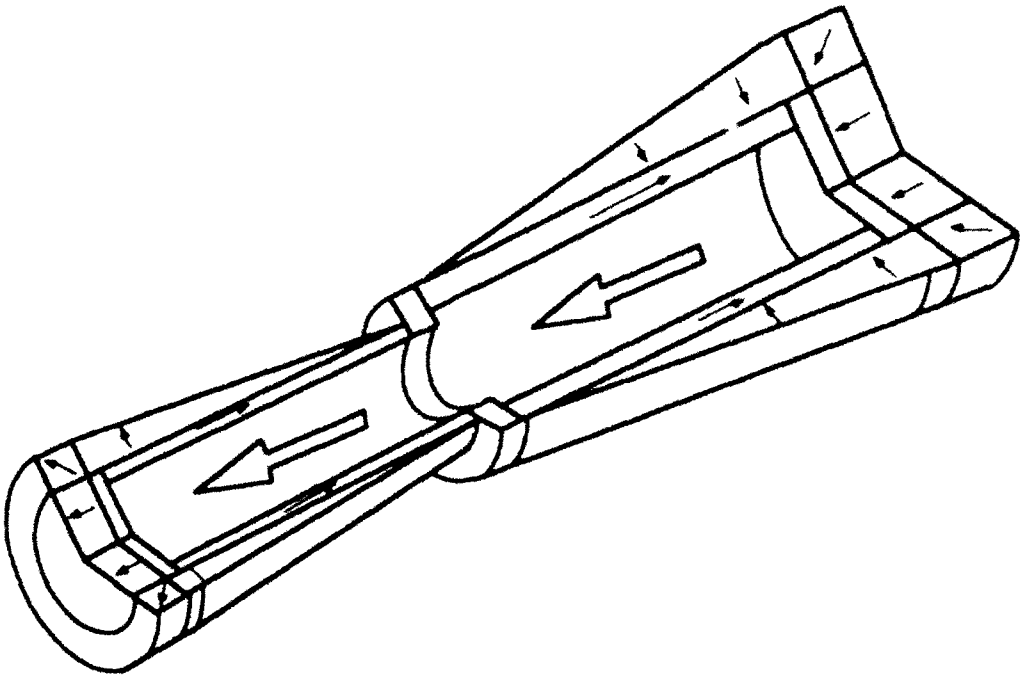

Figure 3. Structure B: The bi-chambered permanent magnet solenoid.

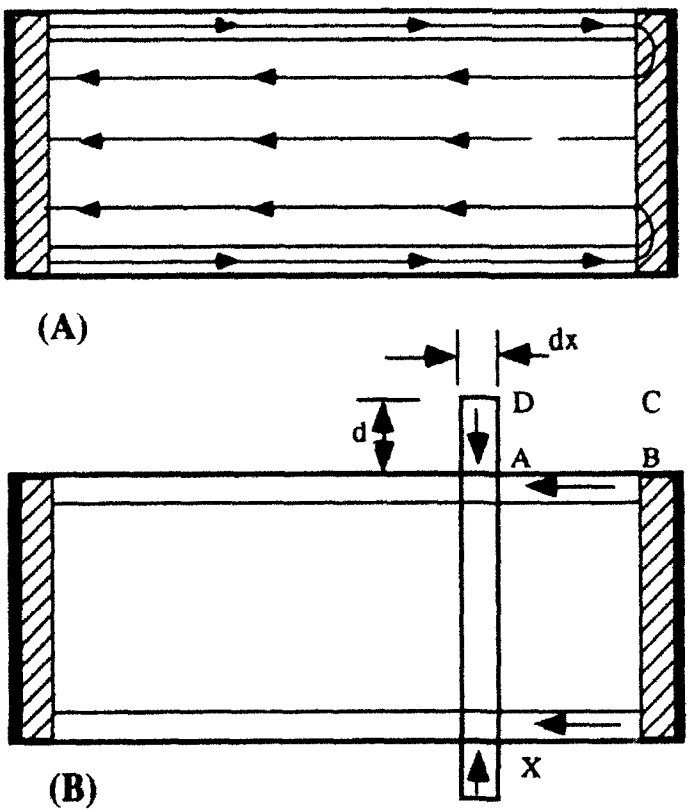

$H_m = H_w$

$B_m A_m = H_w A_w$

$B_m = \mu_R H_m + B_R$

$A_m = A_w/(\mu_R - B_R/|H_w|)$

for $H_w < 0$

$H_c d = H_m X$

$d = H_w X / H_c$

Figure 4. Determination of cladding thickness (A) and supply magnet cross section (B).

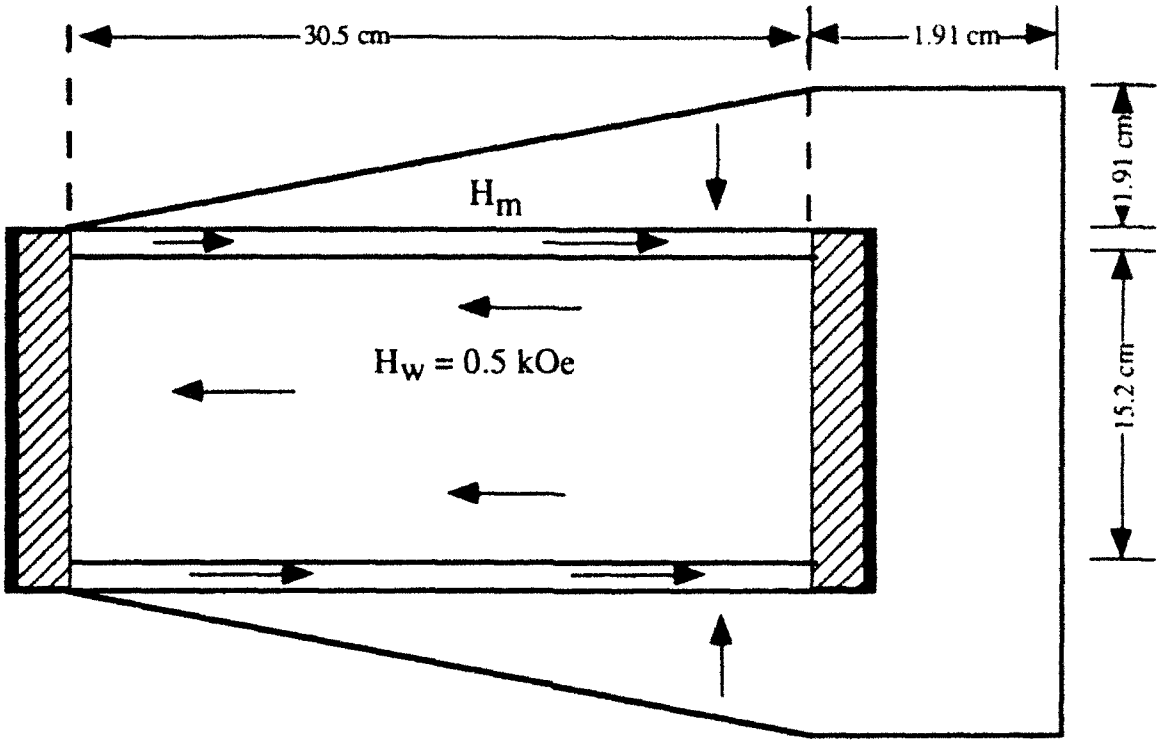

Figure 5. Dimensions fo: mono-chambered device for H_w=0.5 kOe and L=30.5 cm.

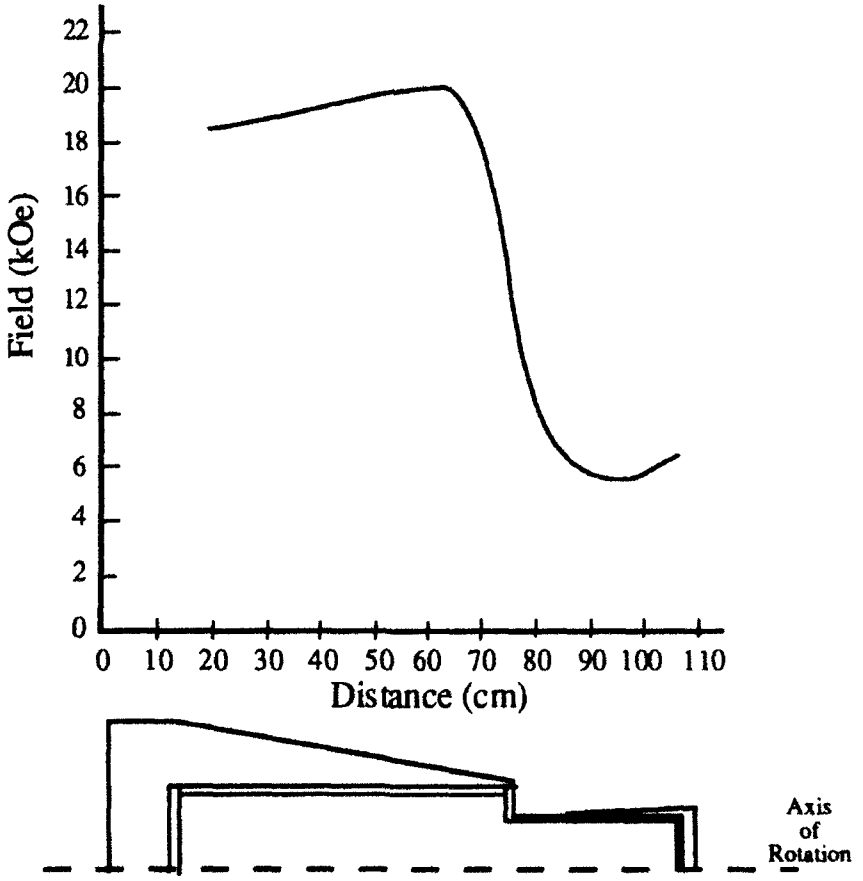

Figure 6. Field profile of a simple uncorrected tandem structure.

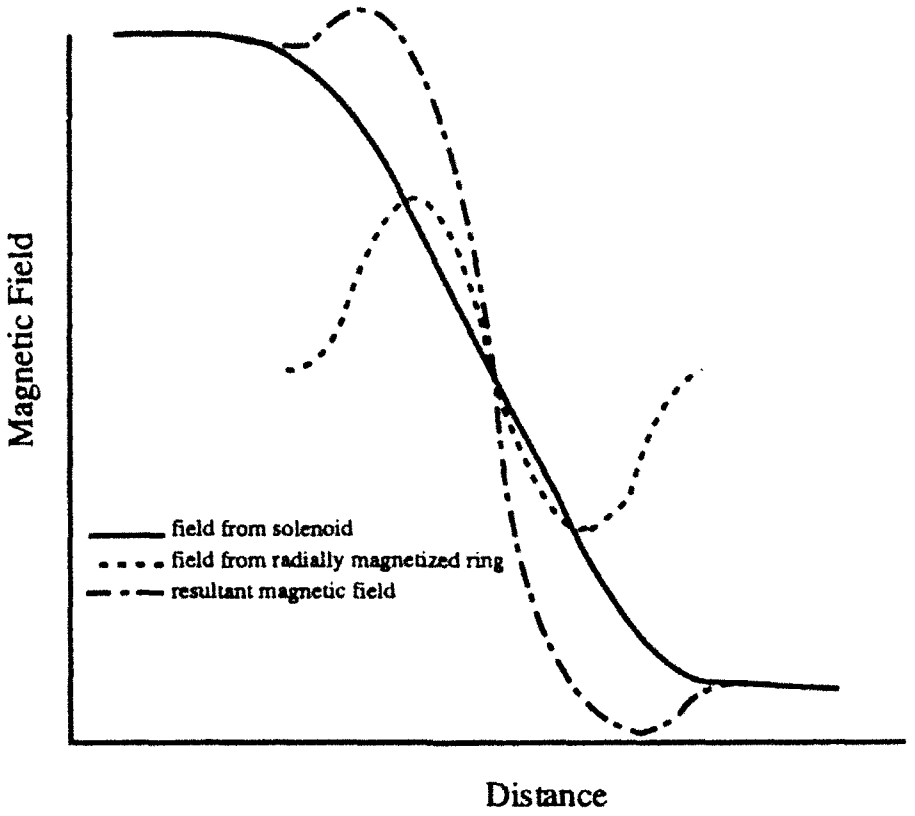

Figure 7. Transition narrowing by placement of a radially magnetized ring at the junction of the bi-chambered device of Figure 3.

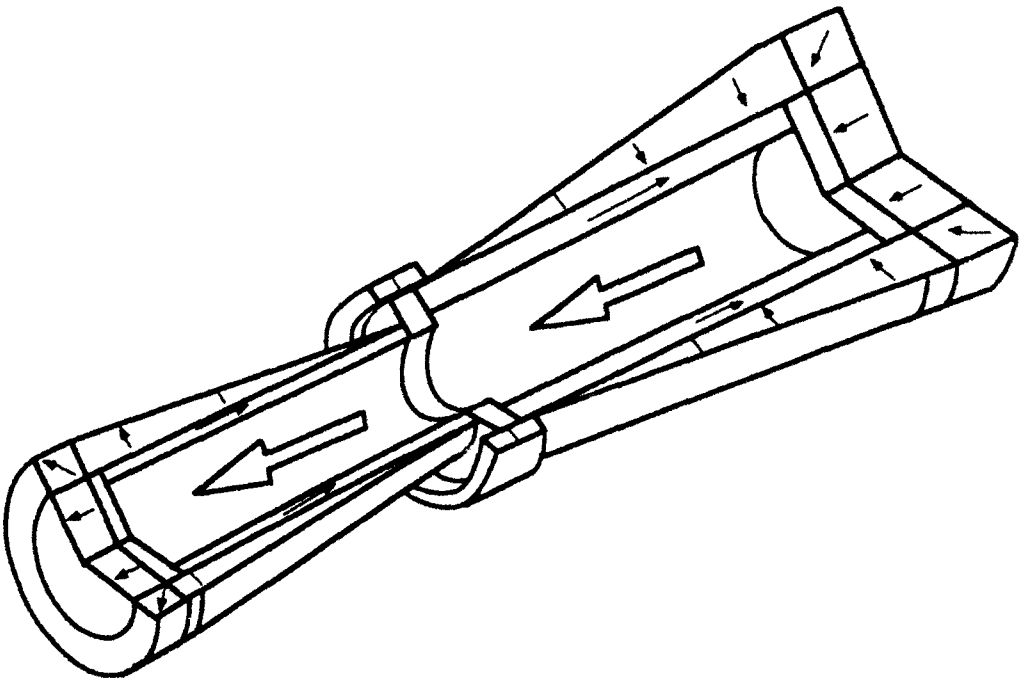

Figure 8. External placement of transition narrowing ring magnet.

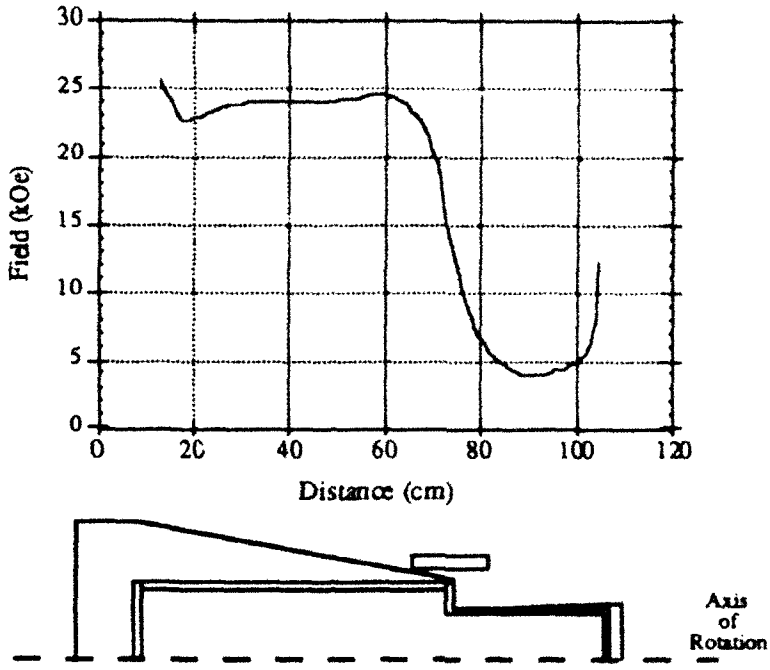

Figure 9. Axial profile of the configuration of Figure 8.

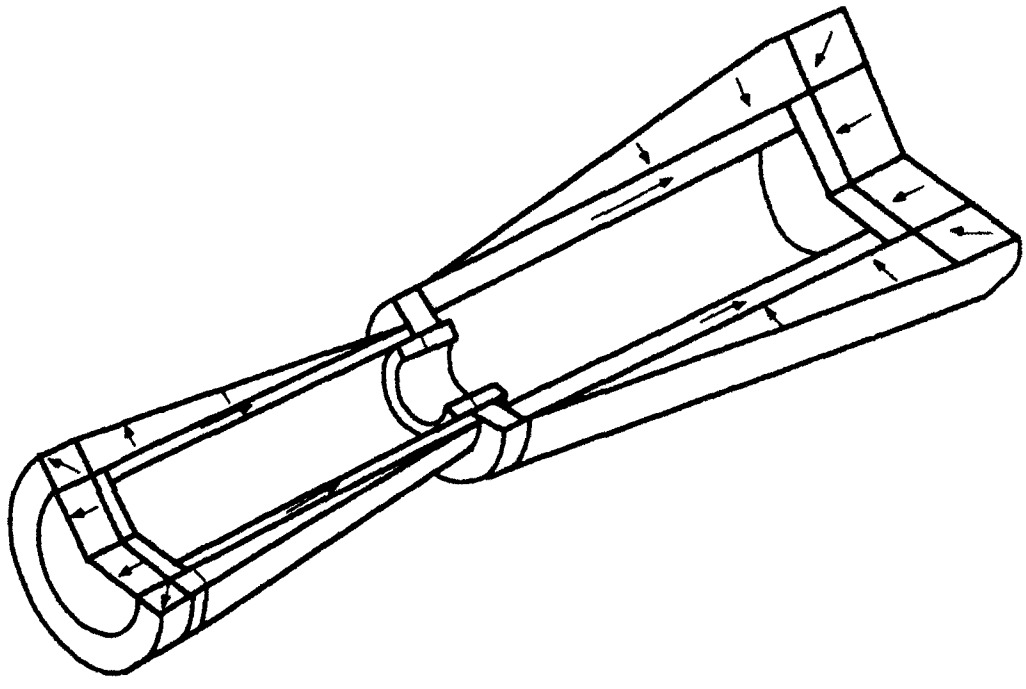

Figure 10. Internal placement of transition-narrowing ring magnet.

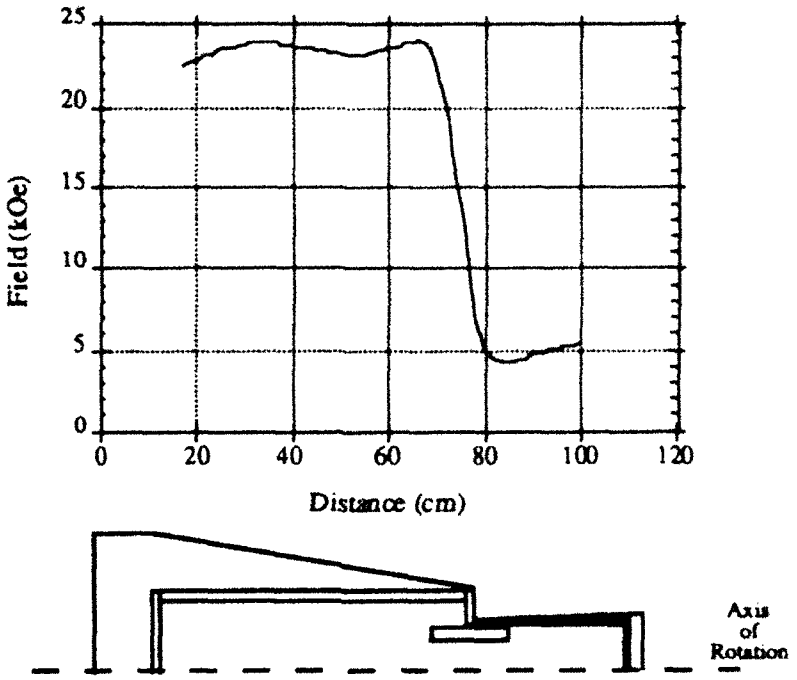

Figure 11. Axial field profile of the configuration of Figure 10.

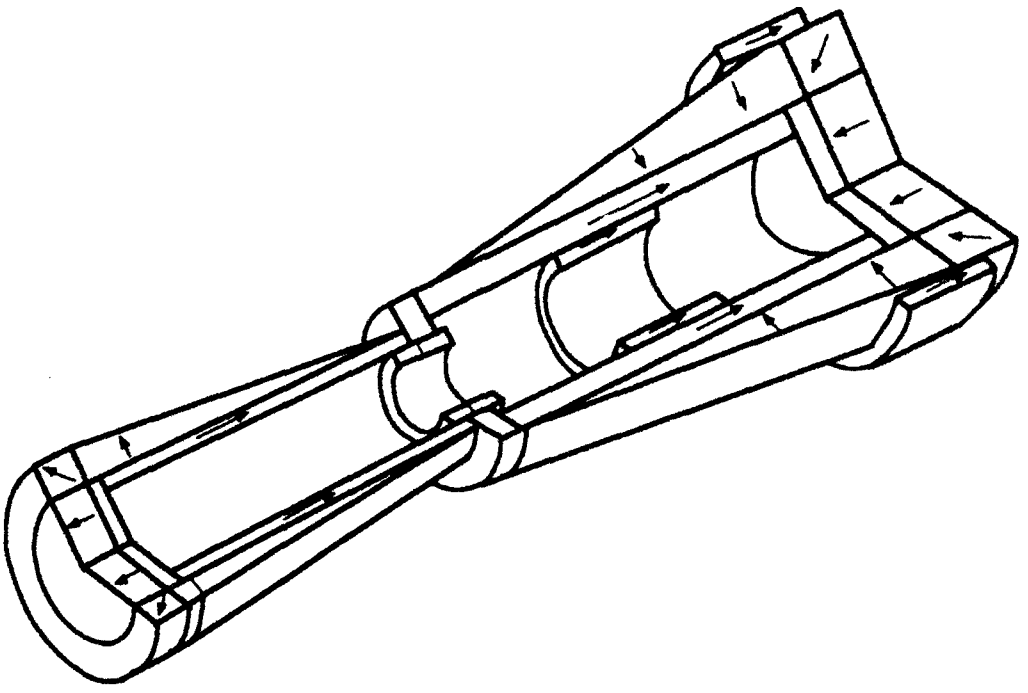

Figure 12. Placement of axially magnetized rings A & B for field smoothing in configuration of Figure 10.

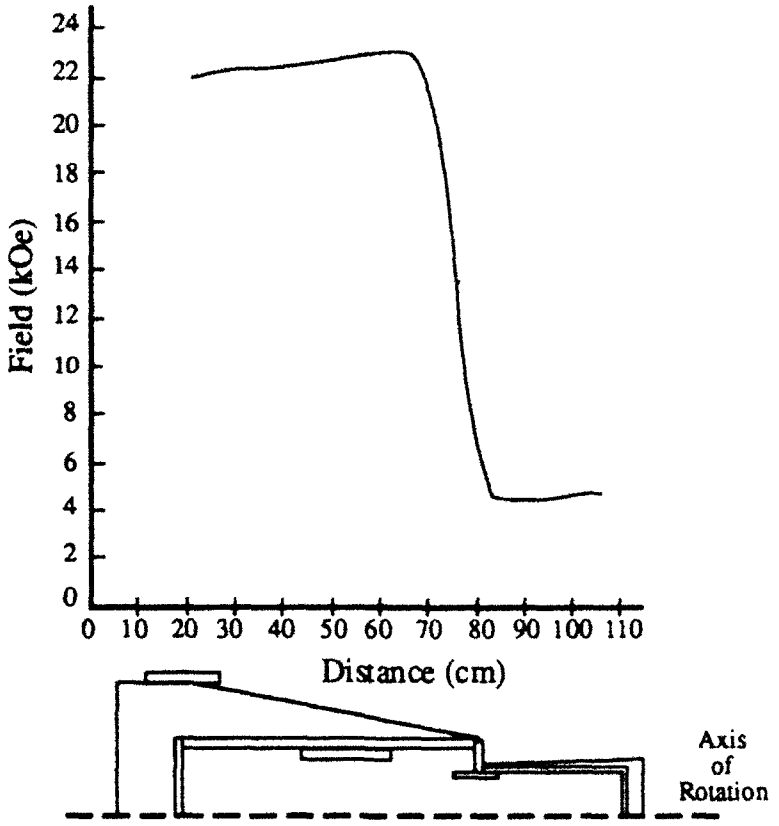

Figure 13. Axial field profile of the configuration of Figure 12.

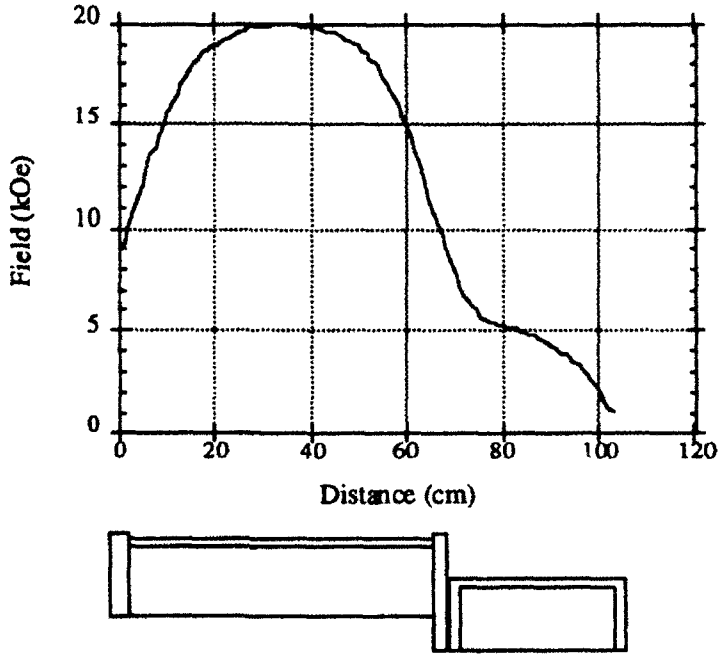

Figure 14. Axial field profile of electric solenoid in Figure 1.

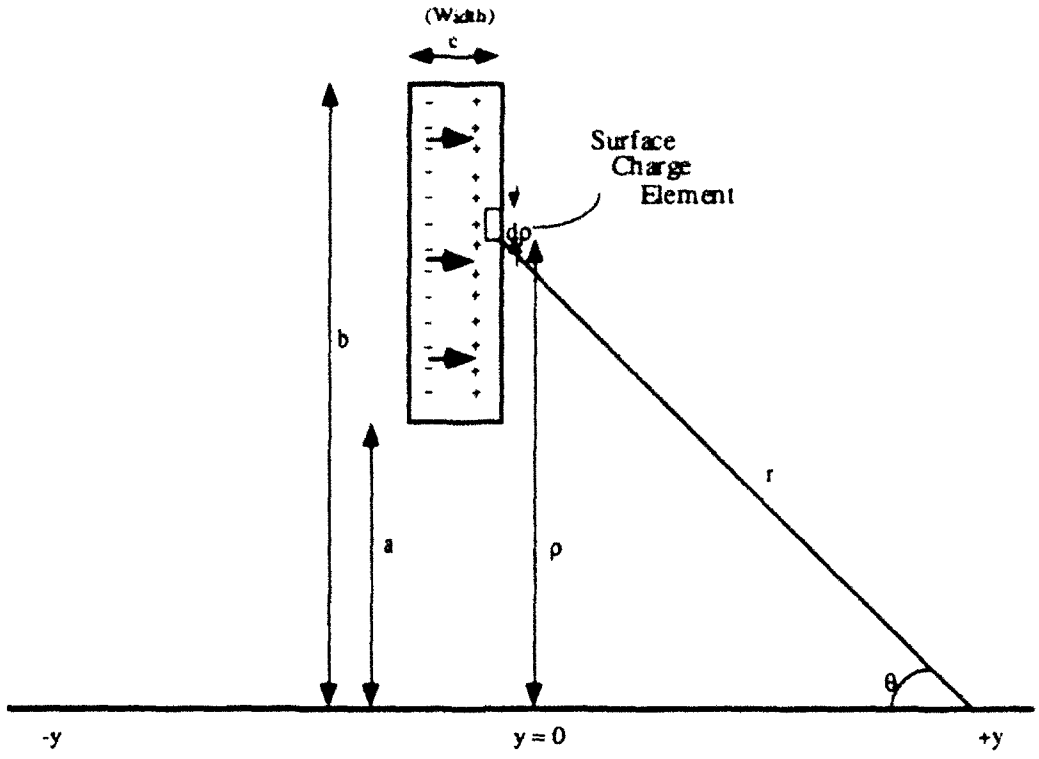

Figure 15. Parameters of an axially magnetized ring.

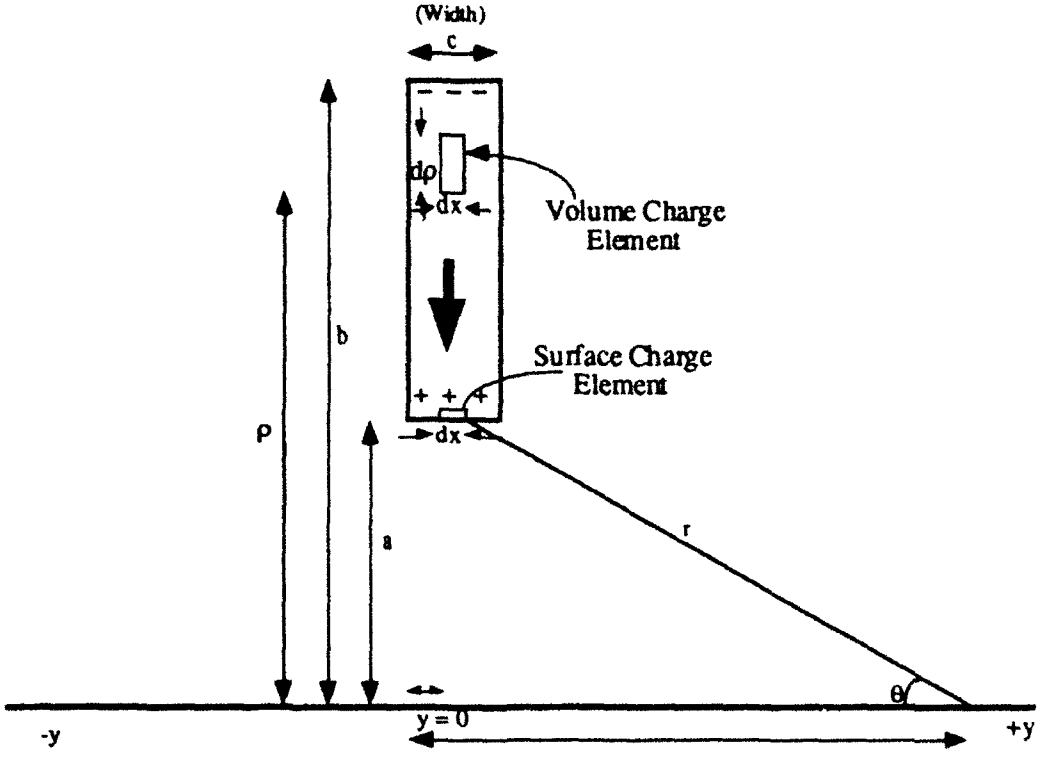

Figure 16. Parameters of radially magnetized ring.

ELECTRONICS AND POWER SOURCES DIRECTORATE
MANDATORY DISTRIBUTION LIST
CONTRACT OR IN-HOUSE TECHNICAL REPORTS

Defense Technical Information Center*
ATTN: DTIC-FDAC
Cameron Station (Bldg 5)
Alexandria, VA 22304-6145

(*Note: Two copies for DTIC will be sent from STINFO Office.)

Director
US Army Material Systems Analysis Actv
ATTN: DRXSY-MP
001 Aberdeen Proving Ground, MD 21005

Commander, AMC
ATTN: AMCDE-SC
5001 Eisenhower Ave.
001 Alexandria, VA 22333-0001

Acting Director
Army Research Laboratory
ATTN: AMSRL-D (Richard Vitali)
2800 Powder Mill Road
001 Adelphi, MD 20783-1145

Deputy Director
Army Research Laboratory
ATTN: AMSRL-DD (COL William J. Miller)
2800 Powder Mill Road
001 Adelphi, MD 20783-1145

Advisory Group on Electron Devices
ATTN: Documents
2011 Crystal Drive, Suite 307
002 Arlington, VA 22202

Commander, CECOM
R&D Technical Library
Fort Monmouth, NJ 07703-5703
1 - AMSEL-IM-IS-L-R (Tech Library)
3 - AMSEL-IM-IS-L-R (STINFO)

Directorate Executive
Electronics and Power Sources Directorate
Fort Monmouth, NJ 07703-5601
1 - AMSRL-EP
1 - AMSRL-EP-T (M. Howard)
1 - AMSRL-OP-RM-FM
22 - Originating Office

Director
Naval Research Laboratory
ATTN: Code 2627
001 Washington, DC 20375-5000

Cdr, PM JTFUSION
ATTN: JTF
1500 Planning Research Drive
001 McLean, VA 22102

Rome Air Development Center
ATTN: Documents Library (TILD)
001 Griffis AFB, NY 13441

Deputy for Science & Technology
Office, Asst Sec Army (R&D)
001 Washington, DC 20310

HQDA (DAMA-ARZ-D/
Dr. F.D. Verderame)
001 Washington, DC 20310

Dir, Electronic Warfare/Reconnais.
Surveillance & Target Acquis. Dir.
ATTN: AMSEL-RD-EW-D
001 Fort Monmouth, NJ 07703-5206

Dir, Reconnais. Surveillance &
Target Acquisition Systems Dir.
ATTN: AMSEL-RD-EW-DR
001 Fort Monmouth, NJ 07703-5206

Cdr, Marine Corps Liaison Ofc
ATTN: AMSEL-LN-MC
001 Fort Monmouth, NJ 07703-5033

Dir, US Army Signals Warfare Dir.
ATTN: AMSEL-RD-EW-OS
Vint Hill Farms Station
001 Warrenton, VA 22186-5100

Dir, CECOM Night Vision &
Electro-Optics Directorate
ATTN: AMSEL-RD-NV-D
001 Fort Belvoir, VA 22060-5677

Cdr, Atmospheric Sciences Lab
LABCOM
ATTN: SLCAS-SY-S
001 White Sands Missile Range, NM 88002

Cdr, Harry Diamond Laboratories
ATTN: SLCHD-CO, TD (in turn)
2800 Powder Mill Road
001 Adelphi, MD 20783-1145